Mutations Affecting the Activity of Toxic Shock Syndrome Toxin-1†

Robert L. Deresiewicz,*,‡,§,∥ JunHee Woo,‡,⊥ Melvin Chan,▽ Robert W. Finberg,∥,▽ and Dennis L. Kasper‡,∥,△

Channing Laboratory, 180 Longwood Avenue, Boston, Massachusetts 02115, Division of Infectious Diseases, Brigham and Women's Hospital, Boston, Massachusetts 02115, Laboratory of Infectious Diseases, Dana-Farber Cancer Institute, Boston, Massachusetts 02115, Division of Infectious Diseases, Beth Israel Hospital, Boston, Massachusetts 02215, and Harvard Medical School, Boston, Massachusetts 02115

Received May 12, 1994; Revised Manuscript Received July 13, 1994⊗

ABSTRACT: Toxic shock syndrome toxin-1 (TSST-1), the potent staphylococcal exoprotein linked to most cases of the toxic shock syndrome, is a V_β-restricted T-cell mitogen (a so-called "superantigen"). TSST-ovine (TSST-O) is a natural variant of TSST-1, and is produced by certain ovine mastitis-associated strains of *Staphylococcus aureus*. Compared to TSST-1, TSST-O is only weakly mitogenic for leporine or murine splenocytes. It differs from TSST-1 at 7 amino acid residues over its 194 amino acid length. Terminus shuffling between the two proteins has suggested that their C-terminal differences (T69, Y80, E132, and I140 in TSST-1; I69, W80, K132, and T140 in TSST-O) are in part responsible for their discrepant mitogenic properties. In order to explore further the functional consequences of altering TSST-1 at residues 132 and 140, we engineered point mutants of TSST-1 at those positions. The mutant proteins were purified to homogeneity from culture supernatants of a nontoxigenic strain of *S. aureus* using a combination of ultrafiltration, liquid-phase isoelectric focusing, and ion-exchange chromatography. The mutants retained global structural integrity as evidenced by circular dichroism spectroscopy, their preserved resistance to trypsin digestion, and their preserved binding to a neutralizing murine monoclonal antibody. The mutants were then tested for mitogenicity for human T-cells: The mutant I140T was approximately as active as wild-type TSST-1, while the mutant E132D was about 10-fold attenuated. On the other hand, the mutants E132A or E132K were each at least 1000-fold attenuated. We conclude that the mitogenic activity of TSST-1 for human T-cells depends critically on the presence and precise position of the negative charge at residue 132.

The toxic shock syndrome (TSS)[1] is an acute multisystem disease characterized by fever, erythroderma, profound hypotension, end-organ failure, and late desquamation. The majority of cases are associated either with colonization or with focal infection by strains of *Staphylococcus aureus* that elaborate an exoprotein called toxic shock syndrome toxin-1 (TSST-1). It is the effect of that exoprotein, either alone or in concert with other factors, that is deemed ultimately responsible in those cases for the clinical syndrome of TSS (Parsonnet & Kasper, 1992).

TSST-1 is single-chain polypeptide of molecular mass ~22 kDa and isoelectric point 7.2 (Blomster-Hautamaa et al., 1986b; Schlievert et al., 1981). It contains no disulfide bonds. It is secreted as mature protein 194 amino acids in length, following cleavage of a 40 amino acid signal sequence. It is a member of a larger group of related pyrogenic staphylococcal and streptococcal exoproteins (Marrack & Kappler, 1990) that have been implicated in a variety of disease processes including staphylococcal food poisoning, staphylococcal scalded skin syndrome, and invasive group A streptococcal infection. All are V_β-restricted T-cell mitogens (i.e., "superantigens"). That is, they stimulate T-cells not according to the epitope specified by the variable region of the T-cell receptor (TCR), but according to the receptor's V_β haplotype.

This activity is believed to be a consequence of the way in which superantigens interact with the cells and molecules of the immune system. They are not taken up and processed like conventional antigens. Rather, superantigens bind directly to a region of the major histocompatibility complex class II molecule (MHC class II) that is on the exterior of the molecule, separate from the normal antigen-binding site. In concert with MHC class II binding, they bind to the solvent-exposed face of the V_β region fo the T-cell receptor, and thus, presumably, activate the T-cell (Marrack & Kappler, 1990).

Much effort has been devoted to defining the regions of TSST-1 that are responsible for its behavior as a V_β-restricted T-cell mitogen. Recent work has been spurred by the discovery of a structural variant of TSST-1 that is produced by certain strains of *Staphylococcus aureus* that cause mastitis in sheep (Lee et al., 1992). This variant, so-called TSST-O (for ovine), differs from TSST-1 at 7 amino acid residues over the 194 amino acid length of the mature protein: T19A, A55T, T57S, T691, Y80W, E132K, and I140T. Compared to TSST-1, TSST-O is only weakly mitogenic for leporine (rabbit) or murine splenocytes. Terminus shuffling between the genes for the two proteins (*tstH* and *tstO*, respectively) at a *Hin*dII/

† This work was supported by Grant 80917 from Tambrands Incorporated (D.L.K. and R.L.D.) and by Grant 91018 from Sandoz Incorporated (R.W.F.).

* Correspondence should be addressed to this author. Telephone: 617-432-2643. Fax: 617-731-1541. E-mail: bobderes@warren.med.harvard.edu.

‡ Channing Laboratory.

§ Brigham and Women's Hospital.

∥ Harvard Medical School.

⊥ Present address: Department of Internal Medicine, Soon Chun Hyang University Hospital, 657 Hanam-dong, Yongsan-ku, Seoul 140-743, Korea.

▽ Dana-Farber Cancer Institute.

△ Beth Israel Hospital.

⊗ Abstract published in *Advance ACS Abstracts,* October 1, 1994.

[1] Abbreviations: TSS, toxic shock syndrome; MHC class II, major histocompatibility complex class II molecule; TSST-1, toxin shock syndrome toxin-1; TSST-O, toxic shock syndrome toxin ovine variant; *tstH*, toxin shock syndrome toxin-1 gene; *tstO*, toxic shock syndrome toxin ovine variant gene; BHI, brain–heart infusion; WT, wild-type; PIEF, preparative isoelectric focusing; IEC, ion-exchange chromatography; CD, circular dichroism.

0006-2960/94/0433-12844$04.50/0

*Hin*cII site that cleaves after codon 62 of the mature proteins has suggested that their C-terminal differences (T69, Y80, E132, and I140 in TSST-1; I69, W80, K132, and T140 in TSST-O) are in part responsible for their discrepant mitogenic properties (Murray et al., 1994).

In order to explore further the functional consequences of altering TSST-1 at residues 132 and 140, we engineered point mutants of TSST-1 at those positions. The mutant proteins were purified to homogeneity from culture supernatants of a nontoxigenic strain of *S. aureus* using a combination of ultrafiltration, liquid-phase isoelectric focusing, and ion-exchange chromatography. The mutants retained global structural integrity as evidenced by circular dichroism spectroscopy, their preserved resistance to trypsin digestion, and their preserved binding to a neutralizing murine monoclonal antibody. The mutants were then tested for mitogenicity for human T-cells: The mutant I140T was approximately as active as wild-type TSST-1, while the mutant E132D was about 10-fold attenuated. On the other hand, the mutants E132A or E132K were each at least 1000-fold attenuated. We conclude that the mitogenic activity of TSST-1 for human T-cells depends critically on the presence and precise position of the negative charge at residue 132.

MATERIALS AND METHODS

Plasmids and Strains. Plasmid pRN6550 contains the intact *tstH* gene on a 1575 base-pair *Mnl*I fragment in the *Nru*I site of pBR322, and was kindly provided by Barry Kreiswirth (Public Health Research Institute of the City of New York, New York, NY). *Bacillus subtilis* strain BD624-(pBD64) was obtained from the Bacillus Genetic Stock Center (Ohio State University, Columbus, OH; Daniel R. Zeigler, Curator). Its plasmid arose as a spontaneous deletion derivative of plasmid pBD12, a hybrid product of the staphylococcal plasmids pUB110 and pC194 (Gryczan et al., 1980). Phage M13mp18 and plasmid pUC19 were purchased from New England Biolabs (Beverley, MA). DNA cloning and single-stranded DNA production were carried out in the Escherichia *coli* strains TG1 [F'*traD36 lacIq* Δ*(lacZ)M15 proA*$^+$*B*$^+$*/supE* Δ*(hsdM-mcrB)*^{5} (r_K-m_K-McrB$^-$) *thi* Δ*(lac-proAB)*] or JM110 [F' *traD36 lacIq* Δ*(lacZ)M15 proA*$^+$*B*$^+$*/ rpsL* (Str^4)*thr leu thi lacY galK galT ara fhuA dam dcm supE44* Δ*(lac-proAB)*]. Toxin production was carried out in *Staphylococcus aureus* strain RN4220, the gift of Jean Lee (Harvard University, Boston, MA).

Oligonucleotides. The M13(–40) primer was purchased from New England Biolabs. All other oligonucleotides used in this study were synthesized on a Model 381A DNA synthesizer (Applied Biosystems, Foster City, CA) and purified with the manufacturer's oligonucleotide purification cartridges.

E. coli Transformation, Maintenance, and Plasmid Recovery. Plasmids were introduced into *E. coli* cells by electroporation, using the Bio-Rad Gene Pulser apparatus (Bio-Rad Laboratories, Richmond, CA) according to the manufacturer's instructions: electrode gap 0.2 cm, electrical field 12.5 kV/cm, capacitor 25 μF, pulse controller 200 Ω, expected time constant 4.5–5 ms. Transformants were selected on Luria–Bertani medium (LB) supplemented with 100 μg/mL ampicillin. Strains stocks were maintained at –80 °C in 33% glycerol. Plasmid DNA was prepared by alkaline lysis according to standard procedures.

B. subtilis Maintenance and Plasmid Recovery. B. subtilis strain BD624(pBD64) was propagated in LB medium supplemented with 0.1% glucose and 50 μg/mL chloramphenicol, and was maintained at –80 °C in 33% glycerol. Plasmid DNA was prepared essentially as it was from *E. coli*, except that the cells were treated with lysozyme at 4 mg/mL prior to the addition of SDS/NaOH.

S. aureus Transformation, Maintenance, and Plasmid Recovery. Shuttle plasmids were introduced into *S. aureus* by electroporation using the method of Pattee (1992), and the following power settings: electrode gap 0.2 cm, electrical field 12.5 kV/cm, capacitor 25 μF, pulse controller 100 Ω, expected time constant ~2.4 ms. The chloramphenicol acetyltransferase marker was induced in the transformants prior to their selection by incubating the cells for 90 min at 37 °C in media containing 0.2 μg/mL chloramphenicol. Transformants were then selected on brain–heart infusion (BHI) plates containing 15 μg/mL chloramphenicol. Strain stocks were maintained at –80 °C in 33% glycerol. Plasmids were transferred from staphylococci back to *E. coli* for analysis using the smash-and-grab procedure: Staphylococcal cells from 1.5 mL of broth culture were pelleted in a microcentrifuge and resuspended in 200 μL of buffer (1% SDS, 2% Triton X-100, 100 mM NaCl, 10 mM Tris, pH 8.0, and 1 mM EDTA); 200 μL of phenol–chloroform and 0.3 g of acid-washed glass beads (average diameter 425–600 μm) were added, and the mixture was agitated at maximum power in a desktop vortex mixer for 3 min. The crude lysate was spun for 5 min, and the aqueous phase was recovered. One microliter was used to electroporate 40 μL of electrocompetent *E. coli* TG1, as described above.

Construction of Staphylococcal Shuttle Plasmid Encoding TSST-1. A tripartite shuttle plasmid for the expression of wild-type or mutant TSST-1 in *S. aureus* was assembled in several steps, as follows:

(A) Generation of a tstH Cassette with Flanking Restriction Sites. The polymerase chain reaction (PCR) was used to create on *Sal*I–*Eco*RI *tstH* cloning cassette. Oligonucleotide primers 5'-GGCCGTCGACTAAAGTCATATTTCACGG-3' and 5'-CCCGAATTCGCGTTATAAAGATAAAAGG-3' were prepared. The first oligonucleotide contains a 4-base leader followed by an *Sal*I site (underlined), and 18 nucleotides identical to a region that begins 370 bp upstream of the *tstH* gene in pRN6550. Its terminal diguanosine (double-underlined) corresponds to the first two nucleotides of the *Bam*HI recognition sequence at position 118 in the map of Blomster–Hautamaa et al. (1986a). The second oligonucleotide also contains a 4-base leader, followed by an *Eco*RI site (underlined), and 19 nucleotides complementary to a region that terminates 82 bp past the end of the TSST-1 coding sequence. The two primers thus define at 1158 bp span of staphylococcal DNA that contains the *tstH* gene as well as enough upstream and downstream sequence (371 and 82 bp, repsectively) to allow it to direct expression of TSST-1 in *S aureus*. Twenty cycles of amplification (denature 94 °C, 1 min; anneal 45 °C, 2 min; polymerize 72 °C, 3 min) were carried out with a Model 480 thermal cycler (Perkin Elmer-Cetus, Norwalk, CT) and the manufacturer's GeneAmp kit as recommended, beginning with 5 ng of pRN6550 template DNA and 100 nmol of each primer. The resultant cassette was cloned between the *Sal*I and *Eco*RI sites of the phage vector M13mp18 to create the recombinant derivative M13mp18.tstH1. PCR fidelity was verified by complete sequencing of the cloned product using the Sequenase kit (US Biochemical, Cleveland, OH).

Oligonucleotide-directed mutagenesis was next used to introduce flanking restriction sites immediately adjacent to the coding region for mature TSST-1. Single-stranded

template DNA was produced from M13mp18.tstH1 and mutagenesis performed with the Amersham Oligonucleotide-Directed In Vitro Mutagenesis Systems according to the manufacturer's instructions (Amersham Corp., Arlington Heights, IL). A *Hin*dIII site was created five nucleotides upstream of the junction between the sequence encoding signal peptide and the sequence encoding mature TSST-1 using the oligonucletide 5′-GCAAAAGCTTCTACAAAC-3′. A *Bcl*I site was created two nucleotides downstream of the *tstH* codon using the oligonucleotide 5′-GCAGAAATTAATTAAT-TGATCACTTTTTCTGTAATA-3′. The new restriction sites are underlined. Candidate mutant clones were screened by restriction analysis. A positive clone was sequenced in its entirety to verify fidelity of the mutagenesis reaction. That mutant phage was designated M13mp18.tstH2.

(B) Assembly of the Shuttle Plasmid. The shuttle plasmid was assembled from DNA from three sources: the *E. coli* vector pUC19 from which the *Hin*dIII site had been deleted, the newly created *Sal*I–*Eco*RI *tstH* cassette from M13mp18. tstH2, and the Gram-positive pBD64.

The *Hin*dIII site of pUC19 was deleted by treating the plasmid sequentially with *Hin*dIII, then with the Klenow fragment of *E. coli* PolI in the presence of excess deoxynucleotides, then with T4 DNA ligase, and then with *Hin*dIII. The altered plasmids were transformed into *E. coli* and the transformants grown in the presence of IPTG, X-gal, and 100 μg/mL ampicillin. White colonies were screened for plasmids that could no longer be cleaved by *Hin*dIII, and one such plasmid was selected for further use. That plasmid was digested with *Sal*I and *Eco*RI, and then ligated to a *Sal*I–*Eco*RI digest of M13mp18.tstH2. The mixture was cloned into *E. coli* and the desired pUC19/*tstH* hybrid identified by restriction analysis. That product, termed pRD1000, was treated with *Eco*RI and with calf-intestinal alkaline phosphatase, and was then ligated to an *Eco*RI digest of pBD64. The adduct was cloned into *E. coli* and the desired shuttle plasmid selected by growing the cells in LB supplemented with 100 μg/mL ampicillin and 15 μg/mL chloramphenicol. Each of the two possible orientations of pBD64 in pRD1000 was obtained, and one was chosen for expression of the TSST-1 point mutants based on its apparently superior level of toxin production. That plasmid was designated pRD1100 (Figure 1).

Construction of Point Mutants of TSST-1. Oligonucleotide-directed mutagenesis was used to change *tstH* codon 132 from glutamic acid (GAA) to either alanine (GCT), aspartic acid (GAC), or lysine (AAA), or to change *tstH* codon 140 from isoleucine (ATA) to threonine (ACT): Single-stranded template DNA was produced from the recombinant phage derivative M13mp18.tstH3, which contains the 672 bp *Hin*dIII–*Eco*RI fragment of pRD1100 fused to M13mp18. Site-directed mutagenesis was performed as described above. Candidate mutant clones were screened by limited DNA sequencing through the region of the desired point mutation. Positive clones were sequenced in their entirety. The altered *Hin*dIII–*Eco*RI fragments were returned to pRD1100 to generate the full-length mutant expression plasmuids pRD1100(E132A), pRD1100(E132D), pRD1100(E132K), and pRD1100(I140T). The mutant expression plasmids were then cloned into *S. aureus* RN4220 by electroporation, as described above. Finally, the mutant expression plasmids were recovered from *S. aureus* and their identities again confirmed by restriction analysis and limited DNA sequencing.

Expression and Purification of Wild-Type or Mutant TSST-1. Wild-type (WT) or mutant TSST-1 was prepared from culture supernatants of *S. aureus* grown in BHI dialysate, and toxin was purified by a combination of ultrafiltration, liquid-phase isoelectric focusing, and ion-exchange chromatography, as follows:

Two hundred fifty milliliters of 5× BHI broth (BHI 185 g/L in pyrogen-free water) was placed into ~60 cm length of dialysis tubing (Spectra/Por 2, MW cutoff 2500, 54 mm diameter; Spectrum Medical Industries, Los Angeles, CA). Air was expelled, and the tube was knotted twice. The tube was placed in a 2-L Erlenmeyer flask along with 625 mL of pyrogen-free water, and the flask and contents were sterilized in an autoclave. After the flask had cooled, 386 μL of chloramphenicol (Cm; 34 mg/mL stock in 100% ethanol) was added, and the mixture was allowed to equilibrate by diffusion. At steady-state, the medium was therefore ~1.4× BHI dialysate and 15 μg/mL Cm. The BHI-containing dialysis tubing "sausage" was left in place.

Two milliliters of an overnight seed culture of *S. aureus* strain RN4220 containing either a wild-type or a mutant TSST-1 expression plasmid was inoculated into the BHI dialysate, and the culture was incubated at 37 °C, 100 rpm, for ~20 h until saturation. The cells were removed by centrifugation, and the supernatant fluid was concentrated to about 40 mL by cross-flow filtration in a Minitan concentrator (Millipore Corp., Bedford, MA) fitted with a 10 kDa ultrafiltration membrane. In the same device, the retentate was washed extensively with water until its total salt concentration was <10 mM as assessed by electrical conductivity.

To the retentate was added glycerol to a final concentration of 10%, pH range 3–10 ampholytes (BioLytes 3/10, Bio-Rad Laboratories) to a final concentration of 2%, and water to a total volume of 55 mL. The mixture was subjected to preparative liquid-phase isoelectric focusing (PIEF) in a Rotofor cell (Bio-Rad Laboratories) at 20 W constant power, with circulating coolant at −15 °C. Following achievement of equilibrium, 20 ~2 mL fractions were collected. The fractions were analyzed by electrophoresis of 30 μL of each in 14% polyacrylamide (SDS/PAGE) followed by staining with Coomassie brilliant blue R-250, according to standard techniques. Positive fractions were pooled, taken to 10% glycerol and a total volume of 55 mL as before, and refocused. Additional ampholytes were not added. Fractions were again analyzed and positive fractions pooled. To disrupt ampholyte–protein aggregates, NaCl was added to a final concentration of 0.5 M and the mixture was stirred at 4 °C for 30 min. Ampholytes and salt were then removed by exhaustive dialysis against 10 mM phosphate buffer, pH 6.15.

The mixture was next subjected to ion-exchange chromatography (IEC) on the cation-exchanger CM-Sepharose CL-6B in an XK 26/40 column (Pharmacia LKB, Piscataway, NJ). Toxin was eluted at room temperature with a 0–300 mM linear gradient of NaCl in 10 mM phosphate buffer, pH 6.15. The elution was monitored by UV absorbance at 280 nm and by electrical conductivity. The fractions containing TSST-1 were combined, washed extensively with pyrogen-free water, and concentrated across a YM-10 ultrafiltration membrane. Between purification of different toxin mutants, the ion-exchange column was purged with 0.1 N NaOH.

Assessment of the Purity of Toxin Samples. Purity of the toxin samples was assessed by SDS/PAGE through 14% polyacrylamide gels, followed either by silver staining or by Western blotting. For silver staining, at least 5 μg of each toxin species was applied per lane, and the gels were stained with the Silver Stain Plus kit (Bio-Rad Laboratories). For

Western blotting, at least 0.5 μg of each toxin species was applied per lane. Immunoreactive bands were visualized by sequential incubation of the blots with polyclonal leporine anti-TSST-1 antiserum (kindly provided by Jeff Parsonett, Dartmouth-Hitchcock Medical Center, Hanover, NH) and 1 μCi of [^{125}I]protein A (Amersham Corp., Arlington Heights, IL), followed by autoradiography overnight at −70 °C using Kodak XRP-1 film (Eastman Kodak, Rochester, NY) and one Cronex intensifying screen. For other experiments, a monoclonal murine anti-TSST-1 antiserum (mAb 8-5-7; the gift of Peter Bonventre, University of Cincinnati Medical Center, Cincinnati, OH) was used in place of the polyclonal leporine antiserum.

Quantitation of Wild-Type or Mutant TSST-1. During the development of our toxin purification scheme and for the determination of the toxin content of crude or partially purified samples, we used the competitive enzyme-linked immunosorbent assay for TSST-1 (TSST-1 ELISA) essentially as described (Parsonnet et al., 1985). TSST-1 samples of known concentration for generation of the standard curves were purchased from Toxin Technology (Sarasota, FL). Those samples had been quantitated by their manufacturer according to the published extinction coefficient of TSST-1, $E^{1\%} = 9.7$ at 277 nm.

Highly purified toxin preparations were quantitated by amino acid analysis using a Beckman Model 6300 amino acid analyzer (Beckman Instruments, Palo Alto, CA) following vapor-phase hydrolysis of the proteins with 6 N HCl. The concentration of toxin in the starting materials was calculated based on the measured mole percent of certain amino acids, on the measured yields of those amino acids, and on the known stoichiometry of the toxins. All determinations were performed at least twice, and the results were averaged.

Circular Dichroism. Circular dichroism (CD) spectroscopy was performed on each of the toxin species using an Aviv Model 62DS circular dichroism spectrometer (Aviv Associates, Lakewood, NJ) and a 0.1 cm path-length quartz cuvette. Scanning parameters were as follows: sample temperature 25 °C, wavelength step size 1 nm, bandwidth 1.5 nm, averaging time 1.0 s, wavelength range 240–190 nm; 10 repetitions. The protein concentrations at which the CD spectra were collected were as follows: WT TSST-1, 200 μg/mL, E132A, 18 μg/mL; E132D, 272 μg/mL; E132K, 241 μg/mL; and I140T, 200 μg/mL, all in water. The CD spectrum of solvent alone was recorded at the beginning and the end of the collection period each day to verify the absence of base-line-drift, and to allow base-line-correction of the experimental scans. Secondary structural predictions were generated by the method of Provencher and Glöckner (1981).

Trypsin Digestion of Wild-Type or Mutant TSST-1. Trypsin sensitivities of wild-type TSST-1 and of the four mutants were compared by incubating 2 μg of each toxin with each of three concentrations of L-1-(tosylamino)-2-phenylethyl chloromethyl ketone-treated trypsin (Sigma Chemical Co., St. Louis, MO) at 37 °C for 20 min in 25 mM Tris, pH 7.5. The reactions were terminated by the addition of phenylmethanesulfonyl fluoride (PMSF) to 1 mM final concentration. The samples were analyzed by SDS/PAGE and Western blotting, using polyclonal leporine anti-TSST-1, as described above.

Lymphocyte Proliferation Assay. Mitogenicity of WT or mutant TSST-1 was assessed in a 4-day lymphocyte proliferation assay using fractionated human peripheral blood leukocytes, as previously described (Deresiewicz et al., 1994). Within a given experiment, all toxin species were assayed in parallel, using peripheral blood leukocytes derived from the same blood donor. Various dilutions of the test toxins were added in quadruplicate to tissue culture wells containing 10^5 irradiated feeders and 10^4 magnetic bead-purified CD4$^+$ T-cells, and the tissue culture plates were incubated for 4 days at 37 °C. Lymphocyte proliferation was assessed by measuring the incorporation of methyl[^{3}H]thymidine on the fourth day. The entire experiment was conducted 3 times, using cells from three different donors.

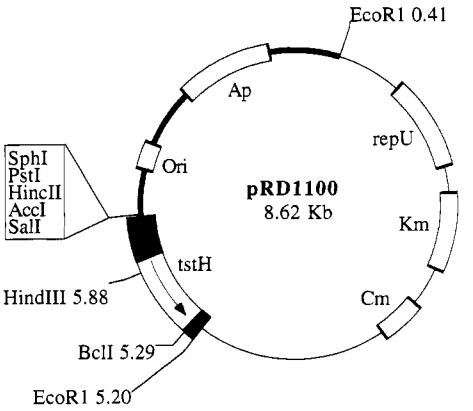

FIGURE 1: Map of pRD1100. pRD1100 consists of three parts: the *E. coli* plasmid pUC19 from which the *Hin*dIII site has been deleted (thick black line), the *B. subtilis* plasmid pBD64 (thin black line), and 1158 bp of staphylococcal chromosomal DNA that begins 370 bp upstream and ends 82 bp downstream of the *tstH* structural gene (very thick segment). The staphylococcal DNA was cloned by PCR, and is flanked by the restriction sties *Sal*I and *Eco*RI. It contains recognition sequences for two other restriction enzymes, *Hin*dIII and *Bcl*I, which were engineered by site-directed mutagenesis. Those sites lie at the junction of the signal sequence with the mature start site (the *Hin*dIII site), and just past the stop codon (the *Bcl*I site). Also shown are Cm, Km, and *repU* for selection and maintenance in *S. aureus*, and Ap and *ori* for selection and maintenance in *E. coli*.

RESULTS

Construction of TSST-1 Expression Plasmid pRD1100. The TSST-1 expression plasmid pRD1100 was created as described above (Figure 1). Complete sequencing of the 1170 bp PCR-generated *tstH* cassette in M13mp18.tstH1 revealed six discrepancies at the nucleotide level relative to the published sequence of *tstH* and its upstream region available at that time (Blomster-Hautamaa et al., 1986a). One of those discrepancies, which was present in each of several independently-derived PCR clones, is here amended for the first time: nucleotide minus-15 relative to the ATG start codon is G rather than T; the T is nucleotide minus-16. Thus, the 16 nucleotides immediately preceding ATG are 5′-TGAAG-GAGAATTAAAA.

pRD1100 was successfully introduced into the nontoxigenic staphylococcal strain RN4220. RN4220(pRD1100) produced ~5–20 mg of TSST-1 per liter of crude culture supernatant as determined by the TSST-1 ELISA and by Western blotting. The quantity of toxin produced from a plasmid having the reverse orientation of the pBD64 portion within pRD1100 was about 2–4-fold lower. No detectable TSST-1 was produced from a fusion plasmid of pBD64 and pUC19 (pRD1200) that lacked the 1170 bp *tstH* PCR cassette.

Construction of Point Mutations in Codons 132 or 140 of tstH. Each of the four desired point mutations in codons 132 or 140 of *tstH* was successfully created by oligonucleotide-directed mutagenesis. The identify of each mutant, and the fidelity of each mutagenesis reaction, was verified by complete sequencing of each mutant cassette in its entirety. The

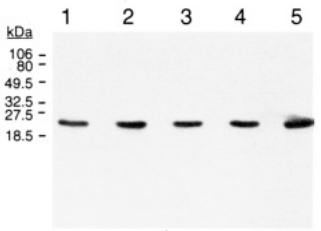

FIGURE 2: Immunoblot of WT or mutant TSST-1 samples. The proteins were subjected to SDS/PAGE, and then electroblotted to nitrocellulose. Immunoreactive bands were visualized by autoradiography following sequential incubation of the blot with murine monoclonal anti-TSST-1 and [^{125}I]protein A. The positions of the molecular mass standards (in kilodaltons) are indicated on the left of the figure. Lane 1, WT TSST-1; lane 2, E132A; lane 3, E132D; lane 4, E132K; lane 5, I140T.

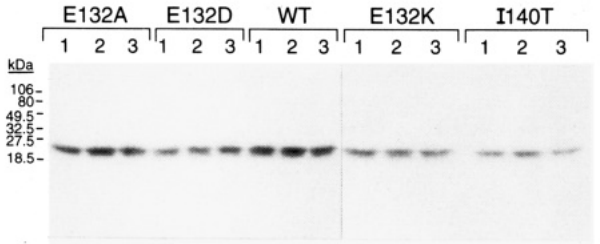

FIGURE 3: Immunoblot of trypsin-treated wild-type or mutant TSST-1. Following trypsinization, the proteins were subjected to SDS/PAGE and electroblotting to nitrocellulose. Immunoreactive bands were visualized by autoradiography after sequential incubation of the blot with leporine anti-TSST-1 antiserum and [^{125}I]protein A. Within each group of three reactions, the trypsin concentrations were as follows: 10 μg/mL (lane 1), 100 μg/mL (lane 2), and 1 mg/mL (lane 3). The positions of the molecular mass standards (in kilodaltons) are indicated on the left of the figure.

mutations were transferred to pRD1100 to give rise to four mutant expression plasmids: pRD1100(E132A), pRD1100-(E132D), pRD1100(E132K), and pRD1100(II40T). The mutant expression plasmids were introduced individually into RN4220. Each derivative strain made abundant immunoreactive product that was easily visualized by Western blotting. No breakdown products were evident. The identity of each mutant was then again verified by retrieval and resequencing of the expression plasmids through the region of their point mutations.

Purification of Wild-Type or Mutant TSST-1. A gentle purification scheme for TSST-1 was developed in order to avoid the possibility of denaturing the mutant toxoids. Although the stability of TSST-1 is well-known, that of its derivatives is less certain. Accordingly, organic precipitation was avoided, and physiologically compatible solutions were used throughout.

Wild-type TSST-1 and each mutant species were purified to homogeneity as described. The overall yield of the purification scheme was ~10–15%. The greatest losses occurred in the PIEF step, during which abundant proteinaceous precipitate was evident. The toxin species eluted from the CM-Sepharose CL-6B ion-exchange column at salt concentrations of between 140 and 170 mM. Species E132A uniquely contained a minor contaminant after one pass over the ion-exchanger, and was therefore subject to peak cutting and a second round of IEC. After that, it too was homogenous.

Purity was documented both by silver and by Western blotting of SDS/PAGE gels. For silver staining, at least 5 μg of each toxin species was used. Each appeared as a single band of the expected molecular weight. Neither extraneous bands not breakdown products were evident (data not shown). For Western blotting, at least 0.5 μg of each toxin species was

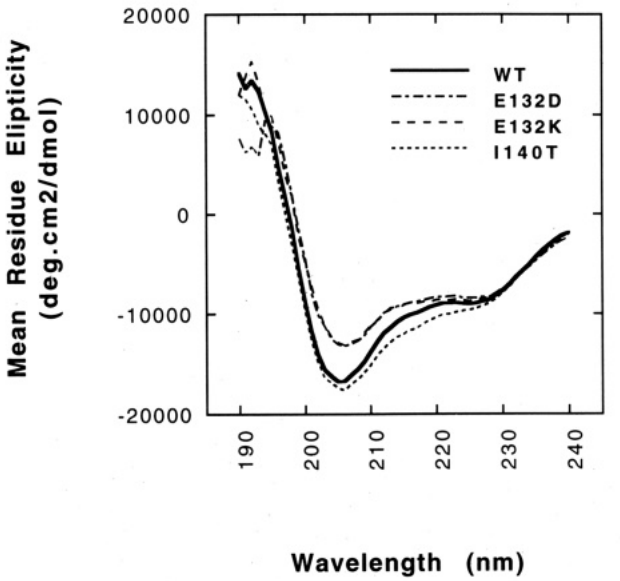

FIGURE 4: Far-UV CD spectrum of wild-type or mutant TSST-1 collected at 25 °C and at protein concentrations of between ~200 and 270 μg/mL in water, as determined by amino acid analysis. The precise concentration at which each protein species was analyzed is lised under Materials and Methods. Scans were base-line-corrected by subtraction of the CD spectrum of water alone. The spectra of E132D and E132K are virtually identical and therefore superimposed. Because the spectrum of E132A was collected at a significantly lower protein concentration than were those of the other species, it had a much more erratic base line. Accordingly, it was not included in this figure.

used, and the blot was probed with polyclonal leporine anti-TSST-1. Again, each protein appeared homogeneous (data not shown).

Quantitation of Wild-Type or Mutant TSST-1. In order most accurately to measure the yield of the WT or mutant TSST-1, each species was subjected to amino acid analysis. Duplicate aliquots of the proteins were hydrolyzed in the vapor phase with 6 N HCl. The constituent amino acids liberated therefrom were then separated and quantitated by high-pressure liquid chromatography (HPLC). The measured mole-percentage of each of 19 amino acids was next compared with its predicted mole-percentage, based on the known stoichiometry of the WT or mutant toxins. Tryptophan was excluded from the analysis, since tryptophan is destroyed by acid hydrolysis. The predicted and measured mole-percentages for the amino acids isoleucine and tyrosine were in good agreement for each of the toxin species, and so subsequent analyses were based on the yields of those two amino acids. The quantity of each protein that had been hydrolyzed initially was next calculated, based on the molar yields of either isoleucine or tyrosine. The two results were averaged. That value was then used to calculate the concentration of protein in the starting material.

Assessment of the Structural Integrity of Wild-Type or Mutant TSST-1. The three-dimensional structural integrity of the wild-type and mutant TSST-1 species was documented in three ways: (i) by demonstrating by immunoblotting the preservation in each of an epitope for a neutralizing mAb; (ii) by demonstrating preservation of their resistance to proteolysis by trypsin; and (iii) by demonstrating the similarity of the morphologies of their circular dichroism spectrographs.

(i) Immunoblotting. To examine the status of an epitope for a neutralizing mAb, 2 μg of each toxin species was separated by SDS/PAGE, blotted to nitrocellulose, and probed with the murine mAb 8-5-7. 8-5-7 has previously been shown capable

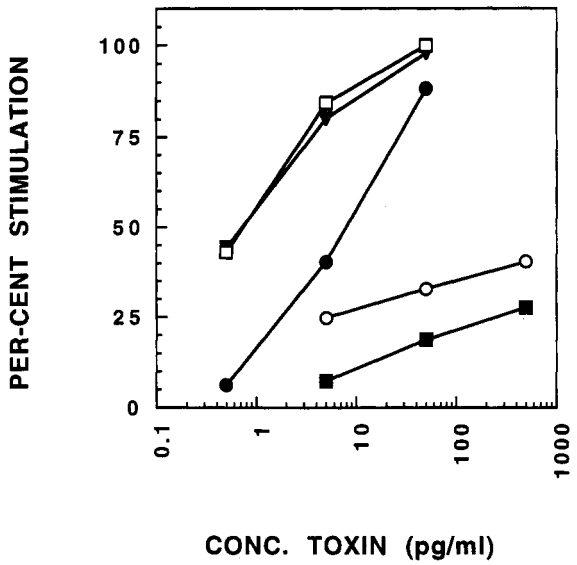

FIGURE 5: Lymphocyte proliferation assay. A total of 10^5 irradiated feeder cells were plated with 10^4 magnetic bead-purified T-cells and with various dilutions of each of the test toxins, as described in the text. Lymphocyte proliferation was assessed by measuring incorporation of methyl[^{3}H]thymidine on the fourth day. The amount of radionucleotide incorporated by the most highly stimulated wells (WT TSST-1 at 50 pg/mL) was defined as 100% stimulation. Data points from the other toxins and dilutions are expressed as percent stimulation relative to those. The results of one representative experiment are shown. WT TSST-1 (□), E132A (■), E132D (●), E132K (○), I140T (▼).

of neutralizing the mitogenicity and the lethality of TSST-1 (Bonventre et al., 1988). All five toxin species were bound by the antibody, and no differences were apparent among them (Figure 2).

(ii) Trypsinization. Despite its content of numerous potential trypsin sites, WT TSST-1 is highly resistant to trypsinization. That resistance is presumably due to the fact that those sites are inaccessible to the protease when the toxin is in its native three-dimensional conformation. To examine if the same holds true for the mutant toxins, 2 μg of WT TSST-1 or of each mutant was treated with trypsin at a trypsin concentration of up to 1 mg/mL. No evident proteolysis was observed for any of the toxin species under any of the concentrations of trypsin tested (Figure 3).

(iii) CD Spectroscopy. To compare the distribution of secondary structural elements in the WT and mutant toxins, their CD spectra were collected in the 190–240 nm range. The spectra were collected at protein concentrations od 200–272 μg/mL, with the exception of E132A's which was collected at 18 μg/mL. The gross morphology of the CD spectra for each of the species was similar (Figure 4), although the base line of the scan of E132A was considerably more erratic than that of the other species (presumably because of the concentration at which it was collected; data not shown). The predicted α-helical contents of the WT toxin and of the mutants E132D, E132K, and I140T ranged from 30 to 40%.

Lymphocyte Proliferation. The mitogenicity of WT TSST-1 and of each of the mutant toxins for human peripheral blood CD4$^+$ T-cells was compared. WT TSST-1 was demonstably mitogenic at 0.5 pg/mL, the lowest concentration at which it was tested. The mutant I140T was approximately as active as WT TSST-1, while the mutant E132D was about 10-fold attenuated. The mutants E132A and E132K were each at least 1000-fold attenuated (Figure 5).

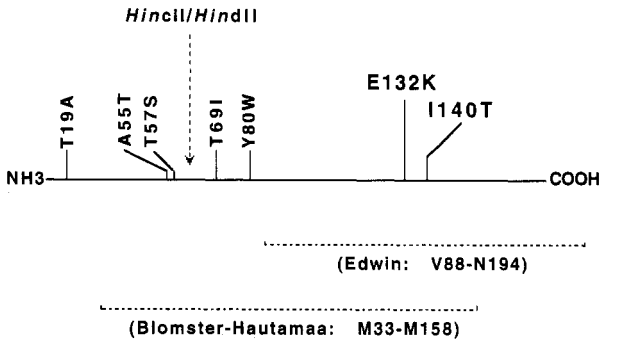

FIGURE 6: Schematic representation of the primary structure of TSST-1. The mature protein consists of 194 amino acids. Blomster-Hautamaa's CN3 fragment (Blomster-Hautamaa et al., 1986b) and Edwin's 12 kDa fragment (Edwin & Kass, 1989) both of which have been implicated in the mitogenic properties of the whole molecule, are indicated by the horizontal dashed lines below the figure. The seven amino acid substitutions that are present in TSST-O are marked above the figure using the one-letter amino acid code. E132 and I140, which were the focus of this study, are bolded. Also shown is the location of the *Hin*cII/*Hin*dII restriction site that cuts both the *tstH* and *tstO* genes after codon 62 of the coding sequences for the mature proteins.

DISCUSSION

Since shortly after the discovery of TSST-1 in 1981, effort has been directed at understanding the structural basis for its behavior as an immunomodulator. That behavior undoubtedly derives both from the three-dimensional structural conformation of the protein and from the chemical properties of the individual residues that remain exposed in that conformation and that are therefore available to interact with the molecules of the immune system. The structure–function investigation can proceed by defining *domains* of the protein that *retain* one or more properties (e.g., mitogenicity, class II reactivity, the ability to compete with whole toxin, etc.), or by defining three-dimensional- structurally-intact *point mutants* of the protein that have *lost* one or more properties. Discoveries of the former type localize the machinery necessary for a given function to a certain domain, while discoveries of the latter type highlight the contribution of the nature and precise positioning of a specific chemical motif on a specific amino acid to the integrity of the overall function. The contribution of that chemical motif might be to orient macromolecules as they dock (e.g., TSST-1 and MHC class II), to make docking of macromolecules energetically favorable, or to transmit some signal from one macromolecule to another.

Early work with TSST-1 concentrated on defining mitogenically active domains of the molecule. Blomster-Hautamaa et al. (1986b) blocked the mitogenic activity of TSST-1 with a monoclonal antibody that recognizes the 14 kDa internal CNBr fragment of TSST-1 (CN3; residues 33–158). Edwin and Kass (1989) demonstrated mitogenicity (attenuated though it was) in the 12 kDa C-terminal pepsin fragment (residues 88–194). These results focused attention on the region between residues 88 and 158 (Figure 6).

Other studies have explored structurally-intact but functionally-attenuated C-terminal point mutants of TSST-1. Blanco et al. (1990) and Bonventre et al. (1993), building on an observation by Kokan-Moore and Bergdoll (1989), showed that the point mutants H135A and H141A each retained the epitope for a neutralizing monoclonal antibody, but were attenuated in mitogenicity. Of the two, H135A was the more severely attenuated, and was also attenuated in the ability to cause lethality in a leporine model of TSS.

Recent work was stimulated by the discovery of TSST-O, a structural variant of TSST-1 that differs from TSST-1 at

7 amino acid residues over the 194 amino acid length of the mature protein (Figure 6), and that is only weakly mitogenic for leporine or murine splenocytes (Lee et al., 1992). Murray et al. (1994) performed terminus shuffling between the genes for the two proteins at a *Hin*dII/*Hin*cII site that cleaves after codon 62 of the mature proteins. That work suggested that the toxins' C-terminal differences are in part responsible for their discrepant mitogenic properties.

In order to explore further the functional consequences of altering TSST-1 at residues 132 and 140, we engineered point mutants of TSST-1 at those positions. We made the change E132A to test the importance of the *presence* of the negative charge at residue 132 for the mitogenicity of TSST-1, and E132D to test the importance of the *position* of the negative charge at residue 132 for mitogenicity. E132K and I140T were made to test the contributions of those substitutions to the overall behavior of TSST-O.

We documented the overall structural integrity of our mutants in three ways: by their preserved binding to a neutralizing murine monoclonal antibody, by their preserved resistance to trypsin digestion, and, in the case of mutants E132D, E132K, and I140T, by the similarity of their CD spectra to that of WT TSST-1. We recognize that the α-helical content for WT TSST-1 that was determined by our CD measurements differs somewhat from the α-helical content that was determined crystalographically, as recently reported (39% vs ~21%) (Acharya et al., 1994). This discrepancy likely reflects the uncertainty inherent in CD predictions of secondary structures of proteins measured to 190 nm, especially for proteins with low overall α-helical content and espcially when a sum-of-structures constraint is included in the analysis (i.e., that the sum of fractions of all secondary structures be 1.0) (Johnson, 1988, 1990). The similarity of the CD spectra of our WT and mutant proteins is significant.

Our mitogenesis assay differs in several important respects from those used by other investigators in this field: (i) the use of CD4+ T-cell responders from human peripheral blood, rather than of murine or leporine splenocytes; (ii) the use of irradiated class II-positive feeder cells that are themselves not capable of proliferating, rather than relying on the viable splenic antigen presenting cells; and (iii) the adjustment of the ratio of feeders to responders such that the stimulation index is maximized (data not shown). We feel that these refinements are advantageous because they ensure that the response being measured is that of the CD4+ T-cell, rather than of other potentially responsive cell types. Moreover, they obviate the risk of a confounding effect of endotoxin, since CD4+ T-cells do not respond to endotoxin (Chilton & Fernandez-Botran, 1993).

We recognize the fact that peripheral blood leukocytes from different donors likely differ in their HLA class II allotype, and may also differ in their relative abundance of CD4+ T-cells bearing certain V_β subtypes. Such donor differences could conceivably influence the results of the proliferation assay. Accordingly, within each trial, all toxin species were assayed in parallel using cells derived from a single donor. The entire experiment was conducted 3 times, with cells derived from different donors used in each repetition. While minor differences in the activity of a given toxin were occasionally noted from one experiment to another, the overall relationships reported here held consistently. The finding of consistent results irrespective of the source of the donor cells strengthens the hypothesis that the differing activities we observed are due to intrinsic differences in the mitogenic properties of the mutants, and are not an artifact of the specific HLA allotype or V_β subtype distribution of the cells against which the mutants were tested.

We compared the activities of the WT and mutant proteins based on the quantity of each required to cause a stimulation equal to half the maximum amount of which the responder cells are capable. The most conservatively changed mutant, E132D, is about 10-fold less active than WT TSST-1. The mutants E132A and E132K are over 1000-fold less active. Thus, both the presence and the precise position of the negative charge at residue 132 are important for the maximal stimulatory activity of TSST-1. It follows that the substitution E132K that exists in TSST-O probably contributes significantly to the attenuated mitogenicity of that protein. Indeed, Murray et al. (1994) created the TSST-O derivative K132E, which can be written as T19A + A55T + T57S + T69I + Y89W + I140T relative to TSST-1. That mutant was mitogenically more active that TSST-O for leporine splenocytes, though still considerably attenuated relative to TSST-1.

The mutation I140T, on the other hand, was not markedly attenuated in our studies and probably does not contribute to the attenuated behavior of TSST-O. This latter result differs from one of Murray et al. (1994) for a mutant that they also referred to as TSST-1 I140T. The discrepancy can be resolved by noting that Murray's mutant was not created directly from *tst*H. Rather, it was made by introducing the change K132E into a TSST-1 N-terminal-to-TSST-O C-terminal fusion that had itself been created by joining the two gene fragments at the *Hin*cII/*Hin*dII site (codon 62 of the mature protein) (Figure 6). Thus, despite the reference to it as I140T, that mutant was evidently actually T69I + Y80W + I140T relative to WT TSST-1. It was attenuated in their hands. Insofar as valid comparisons of mitogenic activity can be made for our mutants and their mutants, which were assayed by slightly different protocols, the discrepancy between the behavior of their species T69I + Y80W + I140T and our mutant I140T provides evidence for an important contribution by residues T69 and Y80, or both, to mitogenicity. Blanco et al. (1990) studied residues in that region of the toxin, and reported that the double mutant Y80A + H82A retains mitogenic activity for unfractionated murine splenocytes comparable to WT TSST-1. Blanco's work was conducted with toxins that were expressed in *E. coli* and recovered in periplasmic extracts, but that were not further purified nor formally quantitated.

Assuming that all the above observations are in fact correct, these data can be reconciled in one of two ways: (i) by concluding that residue T69, but not Y80, contributes to mitogenicity [indeed, T69 is solvent-accessible in the TSST-1 crystal structure, while Y80 is not (Acharya et al., 1994)]; or (ii) by hypothesizing that the double mutant T69I + Y80W is locally perturbed in a way that Y80A + H82A is not, and that that perturbation interferes with mitogenicity. In any case, these observations suggest an area for further study.

By considering all the mutagenesis data together, it seems clear that residues in the region of E132–H141 contribute to the property of mitogenicity. In particular, both the presence and the precise position of the negative charge at residue 132 are important for maximal stimulatory activity. Residues at the N-terminus (T69 and/or others) may also contribute.

ACKNOWLEDGMENT

We gratefully acknowledge Drs. Barry Kreiswirth and Richard Novick for the gift of plasmid pRN6550, Daniel Zeigler and the Bacillus Genetic Stock Center for bacillus strain BD624, Jeffrey Parsonnet for polyclonal leporine anti-

TSST-1, and Peter Bonventre for monoclonal murine anti-TSST-1. We thank Dr. Seong-Eon Ryu for help with circular dichroism spectroscopy, and Drs. R. John Collier and Cameron Ashbaugh for critically reading the manuscript.

REFERENCES

Acharya, K. R., Passalacqua, E. F., Jones, E. Y., Harlos, K., Stuart, D. I., Brehm, R. D., & Tranter, H. S. (1994) *Nature 367*, 94–97.

Blanco, L., Choi, E. M., Connolly, K., Thompson, M. R., & Bonventre, P. F. (1990) *Infect. Immun. 58*, 3020–3028.

Blomster-Hautamaa, D. A., Kreiswirth, B. N., Kornblum, J. S., Novick, R. P., & Schlievert, P. M. (1986a) *J. Biol. Chem. 261*, 15783–15786.

Blomster-Hautamaa, D. A., Novick, R. P., & Schlievert, P. M. (1986b) *J. Immunol. 137*, 3572–3576.

Bonventre, P. F., Thompson, M. R., Adinolfi, L. E., Gillis, Z. A., & Parsonnet, J. (1988) *Infect Immun. 56*, 135–141.

Bonventre, P. F., Heeg, H., Cullen, C., & Chang-Joo, L. (1993) *Infect. Immun. 61*, 793–799.

Chilton, P. M., & Fernandez-Botran, R. (1993) *J. Immunol. 151*, 5907–5917.

Deresiewicz, R. L., Flaxenburg, J. A., Chan, M., Finberg, R. W., & Kasper, D. L. (1994) *Infect. Immun. 62*, 2202–2207.

Edwin, C., & Kass, E. H. (1989) *Infect. Immun. 57*, 2230–2236.

Gryczan, T., Shivakumar, A. G., & Dubnau, D. (1980) *J. Bacteriol. 141*, 246–253.

Johnson, W. C. J. (1988) *Annu. Rev. Biophys. Chem. 17*, 145–166.

Johnson, W. C. J. (1990) *Proteins: Struct., Funct., Genet. 7*, 205–214.

Kokan-Moore, N. P., & Bergdoll, M. S. (1989) *Infect. Immun. 57*, 1901–1905.

Lee, P. K., Kreiswirth, B. N., Deringer, J. R., Projan, S. J., Eisner, W., Smith, B. L., Carlson, E., Novick, R. P., & Schlievert, P. M. (1992) *J. Infect. Dis. 165*, 1056–1063.

Marrack, P., & Kappler, J. (1990) *Science 248*, 705–711.

Murray, D. L., Prasad, G. S., Earhart, C. A., Leonard, B. A. B., Kreiswirth, B. N., Novick, R. P., Ohlendorf, D. H., & Schlievert, P. M. (1994) *J. Immunol. 152*, 87–95.

Parsonnet, J., & Kasper, D. L. (1992) in *Harrison's Principles of Internal Medicine* (Wilson, J. D., Braunwald, E., Isselbacher, K. J., Martin, J. B., Fauci, A. S., & Kasper, D. L., Eds.) Suppl. 1, pp 3–14, McGraw-Hill, New York.

Parsonnet, J., Mills, J., Gillis, Z., & Pier, G. (1985) *J. Clin. Microbiol. 22*, 26–31.

Pattee, P. A. (1992) *Microbiology 610 Laboratory Manual*, 7th ed., revised, Department of Microbiology, Iowa State University, Ames, IA.

Provencher, S. W., & Glöckner, J. (1981) *Biochemistry 20*, 33–37.

Schlievert, P. M., Shands, K. N., Dan, B. B., Schmid, G. P., & Nishimura, R. D. (1981) *J. Infect. Dis. 143*, 509–516.